ORIGINAL ARTICLE

Commensal bacteria drive endogenous transformation and tumour stem cell marker expression through a bystander effect

Xingmin Wang,[1,2] Yonghong Yang,[1,2] Mark M Huycke[1,3]

▶ Additional material is published online only. To view please visit the journal online (http://dx.doi.org/10.1136/gutjnl-2014-307213).

[1]The Muchmore Laboratories for Infectious Diseases Research, Department of Veterans Affairs Medical Center, Oklahoma City, Oklahoma, USA
[2]Department of Radiation Oncology, University of Oklahoma Health Sciences Center, Oklahoma City, Oklahoma, USA
[3]Department of Medicine, University of Oklahoma Health Sciences Center, Oklahoma City, Oklahoma, USA

Correspondence to
Dr Mark M Huycke, Veterans Affairs Medical Center, 921 N.E. 13th Street, Oklahoma City, OK 73104, USA; mark-huycke@ouhsc.edu
Dr Xingmin Wang, University of Oklahoma Health Sciences Center, 1122 N.E. 13th Street Oklahoma City, OK 73117, USA; xingmin-wang@ouhsc.edu

Received 10 March 2014
Revised 13 May 2014
Accepted 15 May 2014

To cite: Wang X, Yang Y, Huycke MM. *Gut* Published Online First: [*please include* Day Month Year] doi:10.1136/gutjnl-2014-307213

ABSTRACT

Objective Commensal bacteria and innate immunity play a major role in the development of colorectal cancer (CRC). We propose that selected commensals polarise colon macrophages to produce endogenous mutagens that initiate chromosomal instability (CIN), lead to expression of progenitor and tumour stem cell markers, and drive CRC through a bystander effect.

Design Primary murine colon epithelial cells were repetitively exposed to *Enterococcus faecalis*-infected macrophages, or purified *trans*-4-hydroxy-2-nonenal (4-HNE)—an endogenous mutagen and spindle poison produced by macrophages. CIN, gene expression, growth as allografts in immunodeficient mice were examined for clones and expression of markers confirmed using interleukin (IL) 10 knockout mice colonised by *E. faecalis*.

Results Primary colon epithelial cells exposed to polarised macrophages or 4-hydroxy-2-nonenal developed CIN and were transformed after 10 weekly treatments. In immunodeficient mice, 8 of 25 transformed clones grew as poorly differentiated carcinomas with 3 tumours invading skin and/or muscle. All tumours stained for cytokeratins confirming their epithelial cell origin. Gene expression profiling of clones showed alterations in 3 to 7 cancer driver genes per clone. Clones also strongly expressed stem/progenitor cell markers Ly6A and Ly6E. Although not differentially expressed in clones, murine allografts positively stained for the tumour stem cell marker doublecortin-like kinase 1. Doublecortin-like kinase 1 and Ly6A/E were expressed by epithelial cells in colon biopsies for areas of inflamed and dysplastic tissue from *E. faecalis*-colonised IL-10 knockout mice.

Conclusions These results validate a novel mechanism for CRC that involves endogenous CIN and cellular transformation arising through a microbiome-driven bystander effect.

Significance of this study

What is already known about this subject?

- Commensal bacteria and innate immunity play a major role in the aetiology of colorectal cancer (CRC). Mechanisms by which commensals drive genomic damage through innate immunity leading to cellular transformation and CRC, however, are lacking.
- *Enterococcus faecalis*, a human intestinal commensal, can polarise macrophages to produce a bystander effect that causes double-stranded DNA breaks, tetraploidy and chromosomal instability (CIN) in target cells and induces inflammation and CRC in interleukin (IL) 10 knockout mice.
- CRC, like other solid tumours, consists of tumour stem cells that are responsible for sustaining tumour growth. We investigated whether *E. faecalis*-polarised macrophages could transform primary colon epithelial cells to cancer-initiating cells.

What are the new findings?

- Exposure of primary colon epithelial cells to commensal-polarised macrophages or 4-hydroxy-2-nonenal, an endogenous mutagen, induces heritable mutagenesis and CIN—features characteristic of CRC. These cells, when transplanted as allografts, grow into poorly differentiated carcinomas.
- Transformed clones show altered expression of three to seven cancer driver genes per clone with increased expression of stem/progenitor cell markers Ly6A and Ly6E. Allografts are strongly positive for the tumour stem cell marker doublecortin-like kinase 1 (Dclk1).
- Dclk1 and Ly6A/E are expressed by epithelial cells in colon biopsies from inflamed and dysplastic tissue in *E. faecalis*-colonised IL-10 knockout mice.

How might it impact on clinical practice in the foreseeable future?

- Understanding mechanisms by which commensals initiate and promote CRC will permit new preventive strategies for decreasing the incidence of this common human cancer.

INTRODUCTION

Sporadic, colitis-associated and inherited forms of colorectal cancer (CRC) arise from somatic mutations and/or epigenetic alterations in tumour suppressors and proto-oncogenes.[1 2] The origin of mutations and epigenetic changes that lead to these cancers, however, remains ill-defined. The initiation of chromosomal instability (CIN) and epithelial cell transformation by the colonic microbiome represents

an endogenous mechanism for driving colon carcinogenesis.[3] Several human commensals produce toxins that damage epithelial cell DNA, increase intestinal barrier permeability, and/or activate T cell responses to promote colorectal carcinogenesis.[4–6] *Enterococcus faecalis* is a human commensal that can drive endogenous mutagenesis leading to CRC in interleukin (IL)-10 deficient mice.[7–9] This commensal polarises macrophages to produce diffusible clastogens (or chromosome-breaking factors) that break double-stranded DNA, disrupt mitotic spindles and generate CIN through a bystander effect (BSE).[8–10]

Commensal-triggered BSE mechanistically links key events in colorectal carcinogenesis to the microbiome. This theory proposes that polarisation of colon macrophages by commensals initiates CIN and transforms colonic epithelial cells through BSE. Colon macrophages are normally quiescent and help maintain immunological tolerance to commensals.[11] These cells, however, are also part of the host defence against invading pathogens and can be polarised to M1 or M2 phenotypes. M1 polarised macrophages secrete proinflammatory cytokines, superoxide and nitrogen radicals in response to infection.[12] In contrast, M2 (or alternatively polarised) macrophages express anti-inflammatory phenotypes that participate in parasite clearance, tissue remodelling and, for tumours, cancer progression.

Colon macrophages ordinarily resist polarisation by commensals, but in the absence of IL-10 can be activated by *E. faecalis* to generate BSE. Using the *Il10*$^{-/-}$ model of CRC, we showed that colon macrophages were polarised to a M1 phenotype by *E. faecalis*.[10] In addition, when colon macrophages were depleted using rectally administered liposomal clodronate, inflammation and CRC were prevented, confirming the essential contribution of these cells to BSE and commensal-driven carcinogenesis.

One mediator for BSE that is produced by *E. faecalis*-infected macrophages is *trans*-4-hydroxy-2-nonenal (4-HNE),[13] a mutagenic breakdown product of ω-6 polyunsaturated fatty acids.[14] This reactive aldehyde is generated in a cyclo-oxygenase (COX)-2 dependent manner and can readily diffuse into neighbouring cells to damage DNA and disrupt mitotic spindles.[13 15] These findings link COX-2, a key target for drugs that prevent CRC,[16 17] with BSE.

The polarisation of colon macrophages by intestinal commensals to generate BSE is a novel mechanism for endogenous CIN and cellular transformation in the adenoma-to-carcinoma sequence.[1 2] We previously showed that a single non-cytotoxic dose of 4-HNE disrupted mitotic spindles and induced tetraploidy in primary colon epithelial cells; one dose, however, failed to produce heritable CIN.[13] In this study, we investigated whether *E. faecalis*-infected macrophages or purified 4-HNE could lead to CIN and cellular transformation in primary colon epithelial cells. Surprisingly, we found that it only took 10 weekly doses of 4-HNE, or exposure to *E. faecalis*-infected macrophages, to produce CIN and transform cells that could grow as poorly differentiated and invasive carcinomas when injected into immunodeficient mice. Gene expression profiling identified networks involving inflammation, cell cycle regulation, proliferation, cancer cell growth and driver genes for cancer.[1 2] Finally, Ly6e, a member of the *Ly6* gene family of haematopoietic stem/progenitor cell markers,[18] and doublecortin-like kinase 1 (Dclk1), a tumour stem cell marker,[19] were upregulated in the colonic epithelium of *E. faecalis*-colonised *Il10*$^{-/-}$ mice. These findings demonstrate that polarised macrophages, or purified 4-HNE, potently induces CIN and cellular transformation in primary colon epithelial cells and validates BSE as a mechanism for endogenous carcinogenesis.

MATERIALS AND METHODS

Cell lines, bacteria, 4-HNE

Young adult mouse colonic (YAMC) epithelial cells (Ludwig Institute for Cancer Research), murine macrophage RAW264.7 cells, and HCT116 human colon cancer cells (American Type Culture Collection) were grown as previously described.[9] YAMC cells proliferate at 33°C in the presence of interferon-γ but not at 37°C in the absence of this cytokine (see below). *E. faecalis* OG1RF was grown as previously described.[9] 4-HNE was purified from infected macrophages as previously described.[13]

Treatment of YAMC cells

RAW264.7 cells were infected with OG1RF at a multiplicity of infection of 1000 as previously described.[8] YAMC cells were co-cultured with *E. faecalis*-infected macrophages, or uninfected macrophages as control, for 72 h in a dual-chamber co-culture system, and recovered for 96 h, as previously described.[8] YAMC cells were dosed with purified 4-HNE at 1 μM for 1 h, which resulted in <5% cytotoxicity as previously reported.[13] Cells were allowed to recover for 1 week and 16 treatment cycles were performed.

Mutant fraction assay

YAMC cells harbour the *H-2K*^{b} class I gene promoter fused to the SV40 *tsA58* early region.[20] As a consequence, cells die by senescence within 10 days when grown at 37°C. Cells acquiring mutations in *tsA58*, however, grow at this temperature. Mutant fractions were assayed following every other treatment and compared with controls as previously described with slight modification.[20] In brief, 1×10^{5} cells were seeded with complete RPMI 1640 medium in the absence of interferon-γ at 33°C overnight to allow adherence. Cells were incubated at 37°C for 10 days. Randomly selected colonies were expanded. Remaining colonies were fixed, stained and used to calculate mutant fractions. Data were expressed as means with the SD. Student t test was used for comparison between experimental groups and controls. Analysis of variance was used for multiple comparisons. p Values <0.05 were considered statistically significant.

Fluorescent-activated cell sorting

Ploidy assays were performed as previously described.[9] Mitotic cells were stained with phosphorylated histone 3 antibody (Cell Signaling Technology) and DNA contents were determined by propidium iodide staining. Ly6A/E expression by cells was assessed using fluorescein isothiocyanate (FITC)-conjugated rat antimouse Ly6A/E antibody (BD BioSciences).

Fluorescence in situ hybridisation

Two-color fluorescence-labelled probes were used to detect mouse chromosomes 11 and 18 according to manufacturer's instructions (Applied Spectral Imaging). Metaphase plates were prepared as previously described.[9] Images were collected by fluorescence microscopy (Nikon).

In vitro transformation

Anchorage-independent growth was determined by spheroid formation in soft agar using CytoSelect 96-well Cell Transformation Assay, Cell Recovery Compatible Kit according to manufacturer's instructions (Cell Biolabs). Randomly selected single clones were recovered from soft agar using a matrix solubilisation solution and then grown in RPMI 1640 without interferon-γ at 37°C and expanded in RPMI medium with 10% fetal bovine serum prior to allografting.

Allografts

Animal studies were approved by the Institutional Animal Care and Use Committees at the University of Oklahoma Health Sciences Center and Oklahoma City Veterans Affairs Medical Center. For allografts, 1×10^6 cells for clones derived from treatments with polarised macrophages or 4-HNE were either directly subcutaneously injected into the flanks of 6-week-old female NOD/*scid* mice (Jackson Laboratory) or injected after mixing with matrigel (BD Biosciences). Untreated YAMC and HCT116 colon cancer cells served as negative and positive controls, respectively. Tumour masses were resected when flank masses reached 10% of body weight or at 20 weeks postengraftment and fixed in 10% formalin.

Staining

Immunohistochemical and immunofluorescent staining of allografts and colon biopsies were performed as previously described.[21] Cytokeratins, Ly6A/E and Dclk1 were stained using mouse anti-pancytokeratin monoclonal antibody (Novus Biologicals), rat anti-Ly6A/E (BD BioSciences) and rabbit polyclonal antibody to Dclk1 (Abcam). Rabbit anti-nitric oxide synthase 2 (Enzo Life Sciences), anti-arginase 1 (Sigma), and anti-MSH2 (Santa Cruz Biotechnology) polyclonal antibodies were used for Western blots.

Gene expression

Total RNA was extracted from clones and YAMC cells using AllPrep DNA/RNA/Protein Mini Kit (Qiagen). Gene expression microarrays were performed using Mouse WG-6 v2.0 Expression BeadChip according to manufacturer's instructions (Illumina). Differentially expressed genes were screened using a 5% false discovery rate. Gene expression was compared for each clone and compared with averages for controls. Genes with the greatest degree of differential expression were further analysed by averaging all transformed clones and comparing results with control averages using $p<0.001$. Response networks were analysed by Ingenuity Pathways Analysis software (Qiagen).

RESULTS

E. faecalis-infected macrophages and 4-HNE cause mutations

E. faecalis-infected murine macrophages (RAW264.7) strongly expressed inducible nitric oxide synthase 2 and did not express arginase 1 (figure 1A). In addition, our previous study showed substantial TNFα production in supernatants of *E. faecalis*-infected macrophages,[21] indicating M1 polarisation of RAW264.7 cells by *E. faecalis*. To evaluate the mutagenic potential of *E. faecalis*-polarised macrophages, we initially exposed YAMC cells to infected macrophages using *tsA*58 as a target for mutagenesis. Mutant fractions increased significantly after only four treatments compared with cells co-cultured with uninfected macrophages (figure 1B, $p<0.01$). The highest mutant fractions occurred after 10 treatments (56.8 ± 10.6 per 1×10^5 cells). To determine the role of 4-HNE—a diffusible endogenous mutagen, clastogen and spindle poison produced by polarised macrophages[13 15]—we exposed YAMC cells to 1 μM 4-HNE for 1 h once a week. Compared with shams, 4-HNE-treated cells showed significantly increased mutant fractions after six doses with peak fractions occurring after 12 treatments (311.3 ± 18.3 per 1×10^5 cells, $p=0.02$; figure 1C). Of note, the fractions steadily decreased after 12 treatments for *E. faecalis*-infected macrophages and 14 treatments with 4-HNE (figure 1B,C), possibly due to accumulating mutations leading to cell death and/or senescence. These data show that, up to a point, repetitive in vitro exposure of primary epithelial cells to *E. faecalis*-polarised macrophages or 4-HNE causes cumulative genotoxicity.

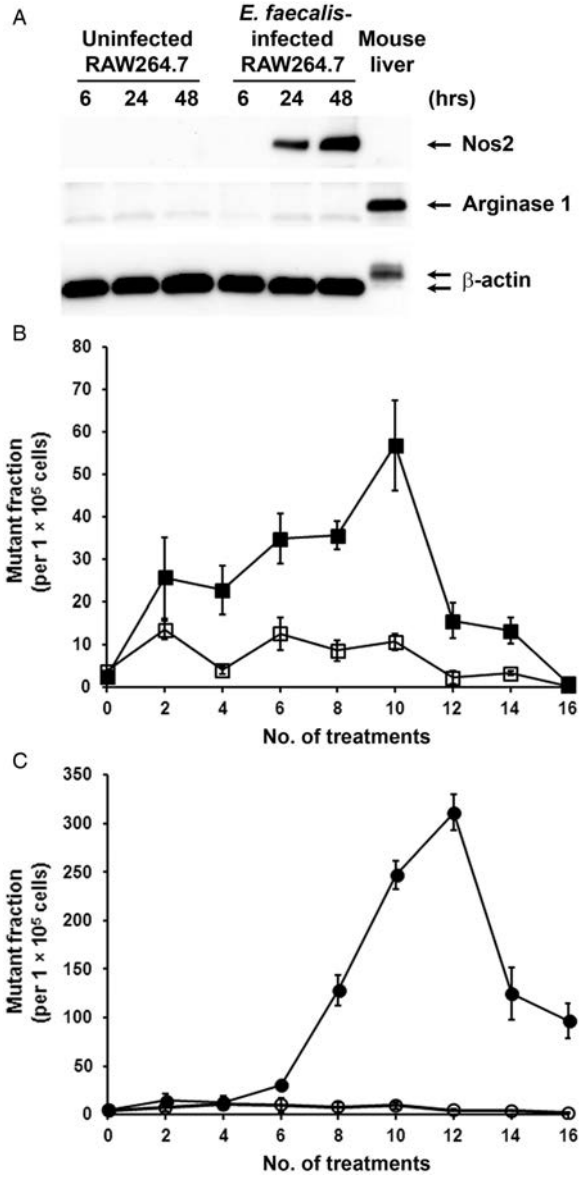

Figure 1 *Enterococcus faecalis*-infected macrophages and 4-hydroxy-2-nonenal (4-HNE) are mutagenic to primary colon epithelial cells. (A) Western blotting shows expression of nitric oxide synthase 2 (Nos2), but not arginase 1, in RAW264.7 cells after infection with *E. faecalis*, indicating M1 polarisation. (B) Mutant fractions for *tsA*58 significantly increase following weekly exposure of YAMC cells to *E. faecalis*-infected macrophages (*closed squares*) compared with uninfected macrophages (*open squares*). (C) Mutant fractions for *tsA*58 also increase following eight weekly treatments with 1 μM 4-HNE (*closed circles*) compared with untreated controls (*open circles*).

E. faecalis-infected macrophages and 4-HNE induce aneuploidy and CIN

Aneuploidy and CIN are common features of CRC.[22] We previously showed that a single exposure of YAMC cells to *E. faecalis*-infected macrophages was unable to produce aneuploidy or tetraploidy,[9] possibly due to robust cellular defence and repair mechanisms. To determine whether repeated

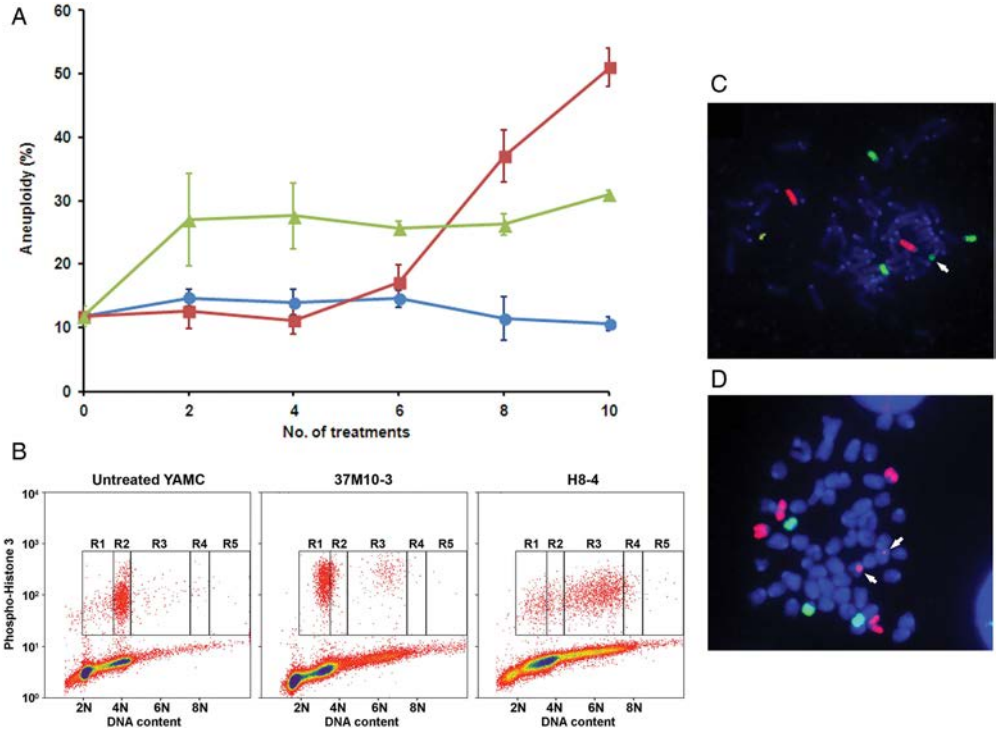

Figure 2 *Enterococcus faecalis*-infected macrophages and 4-hydroxy-2-nonenal (4-HNE) induce aneuploidy and chromosomal instability (CIN) in primary colon cancer cells. (A) After 8 weekly treatments, the rate of aneuploidy significantly increases in YAMC cells co-cultured with *E. faecalis*-infected macrophages (*red squares*) compared with untreated control (*blue circles*). The proportion of aneuploid cells increases after only two treatments with 1 μM 4-HNE (*green triangles*). (B) Representative histograms of mitotic cells by fluorescent-activated cell sorting show increased numbers of aneuploid cells (R1 and R3 windows) in YAMC clones isolated after 10 treatments with *E. faecalis*-infected macrophages (37M10-3, *middle*) and 8 treatments with 4-HNE (H8-4, *right*) compared with sham-treated cells (*left*). (C) and (D), fluorescence in situ hybridisation analysis shows aberrant karyotypes with chromosomal translocations (*arrows*). *Red*, chromosome 11; *green*, chromosome 18.

exposures could produce CIN, we analysed YAMC cells exposed to *E. faecalis*-polarised macrophages or 4-HNE by fluorescent-activated cell sorting. Compared with shams, we found significantly increased percentages of aneuploid cells after repetitive treatment using either modality (figure 2A, $p<0.001$ and $p<0.01$, respectively).

To determine whether these treatments generated heritable CIN, we analysed cells for ploidy. Clones were generated by expanding single cells at 37°C after 6–10 treatments with either *E. faecalis*-infected macrophages or purified 4-HNE. Eighteen of 22 clones (82%) displayed an aneuploid karyotype (table 1 and figure 2B). In addition, fluorescence in situ hybridisation showed numerous chromosome translocations, indicating CIN (figure 2C,D). To determine whether MSH2, a mismatch repair gene commonly implicated in CRCs with microsatellite instability (MIN), was altered in clones, we performed Western blotting for this protein. Increased MSH2 expression was noted compared with controls (see online supplementary figure S1), suggesting that this form of genomic instability was unlikely in these clones.

Cellular transformation

Anchorage-independent growth is a hallmark of cellular transformation. To investigate whether repeated exposure of YAMC cells to *E. faecalis*-infected macrophages or 4-HNE led to this phenotype, we tested cells for growth in soft agar after every two treatments. Untreated cells failed to grow in soft agar while treated cells showed anchorage-independent growth (figure 3A).

To further assess the oncogenic and transformation inducing abilities of *E. faecalis*-polarised macrophages or 4-HNE, we engrafted 25 clones into the flanks of NOD/*scid* mice. Injection of HCT116 human colon cancer cells (as controls) resulted in large tumours (see online supplementary figure S2). No tumour growth was noted for YAMC cells and no clone, except M17 (see online supplementary figure S3A–D), formed tumours when injected directly into mice. However, when clones were premixed with matrigel, 10 of 25 clones developed flank masses (table 1, figure 3B). Of note, all were derived from clones exposed to at least 10 treatment cycles. Eight of 10 masses were poorly differentiated carcinomas (figure 3C) with 3 tumours invading skin and/or muscle (see online supplementary figure S3E,F). One mass was lymphoid and may represent a spontaneously formed neoplasm known to develop in NOD/*scid* mice.[23] Immunohistochemical staining using a pan-keratin reagent confirmed 8 of 10 flank masses as epithelial in origin (figure 3D). Staining of each carcinoma was also positive for Dclk1 (figure 3E). Finally, these tumours were verified as being derived from YAMC cells by amplifying the gene for SV40 large T antigen (figure 3F). For clones H3 and 37M10-3, weakly positive PCRs likely represented a small number of transformed YAMC cells that had persisted within larger flank masses. In aggregate, these findings indicated that exposure of a primary colon epithelial cell line to commensal-polarised macrophages or to 4-HNE resulted in clones that grew as poorly differentiated invasive carcinomas expressing the tumour stem cell marker Dclk1.

Gene expression in transformed clones

To explore gene expression associated with cellular transformation, whole-genome profiling was performed on 10 transformed clones. Expression data were normalised and

Table 1 Genomic instability and tumour growth for YAMC clones and control cell lines

Treatment, cell lines and subclones	Number of treatments*	Cells with aneuploidy and tetraploidy (%±SD)†	Tumour size (mm^3)	IHC staining for keratins‡	Histopathology of tumours
Untreated					
HCT116	None	ND	1751	+	Poorly differentiated carcinoma
YAMC	10	10.6±3.5	–		
Treated with 4-hydroxy-2-nonenal					
H1	10	23.8	–		
H2	10	24.2	61	+	Poorly differentiated carcinoma
H3	10	13.2, 11.8	30	–	Acute/chronic inflammation
H4	10	30.5±4.7	–		
H5	10	16.1±4.9	201	+	Poorly differentiated carcinoma
H6	10	22.6	–		
H7	10	33.8±9.2	195	+	Poorly differentiated carcinoma
H8	10	18.9, 24.4	–		
H8-1	8	40.7±13.9	–		
H8-4	8	90.8	–		
H9	10	26.9, 16.6	–		
Exposed to *Enterococcus faecalis*-infected macrophages					
37M10-1	10	17.5±8.7	–		
37M10-3	10	22.8, 38.0	54	–	Lymphoid mass
37M10-5	10	77.0±13.5	–		
37M10-6	10	31.1±13.3	–		
37M10-7	10	77.3	–		
M3	10	8.4	62	+	Poorly differentiated carcinoma
M11	10	ND	584	+	Poorly differentiated carcinoma invading skin
M12	10	ND	–		
M13	10	ND	661	+	Poorly differentiated carcinoma
M14	10	84.9±19.3	–		
M15	10	32.3±8.4	1117	+	Poorly differentiated carcinoma invading skin
M16	10	21.3	–		
M17	10	30.1	74	+	Poorly differentiated carcinoma invading muscle
M6-1	6	33.4	–		

*YAMC cells were fed twice a week and subcultured once a week for 10 successive weeks.
†Average and SD calculated for experiments repeated ≥3 times. For experiments with <3 repeats, percentages listed for each individual experiment.
‡See materials and methods for immunohistochemical (IHC) staining using a pan-keratin reagent.
ND, not determined; +, positive staining in cancer cell cytoplasm; –, negative staining.

comparisons made with untreated YAMC cells. Hierarchical clustering was performed for 11 000 of the most variable probes and correlations established using two controls (r=0.9), four clones from 4-HNE treatments (r=0.4–0.7) and six clones from polarised macrophage treatments (r=0.3–0.5). We filtered these probes down to 2391 that had at least a twofold change compared with controls and identified 1974 differentially expressed genes (figure 4A). Of these, 567 genes were unique for 4-HNE generated clones, 688 for macrophage induced clones and 719 that were shared by all 10 transformed clones. Compared with controls, each transformed clone contained three to seven cancer driver genes (table 2).[2] Finally, Dclk1 was not differentially expressed in any clone.

To identify response networks, we averaged gene expression for these same 10 transformed clones and compared the results with untreated YAMC cells. There were 151 significantly differentially expressed genes of which 62 were upregulated and 89 downregulated (see online supplementary table S1). Ingenuity pathway analysis identified eight response networks (see online supplementary table S2). The first ranked network contained 25 genes involved in infectious diseases and cell morphology (figure 4B). Other networks included cell cycle regulation, cell growth and proliferation, and cancer development (see online supplementary table S2). Finally, several gene regulators were identified including Mapk1, Ifna2, Trim24, IfnG and Trp53.

Stem/progenitor and tumour stem cell markers

Ly6 genes code for haematopoietic stem/progenitor cell markers that are expressed in diverse cancers.[18] *Ly6e* showed strong upregulation in nearly all transformed clones (average fold-change (±SD), 8.39±2.40 and 7.96±1.97 for each probe). In addition, *Ly6a* expression was also increased (average fold-change of 16.8 ±8.33 for one probe) (figure 5A). To confirm these data, we assayed transformed clones for Ly6A/E by fluorescent-activated cell sorting and compared results with untreated YAMC cells. We found that the percentage of positive cells was significantly increased for these surface markers in all clones except H5 (42.1 ±18.7 vs 7.4±2.6, p<0.001 by analysis of variance) (figure 5B, C). In addition, Ly6A/E-positive cells were noted in allografts (figure 5D, *left* and see online supplementary figure S4A). Compared with sham-colonised *Il10*$^{-/-}$ mice, Ly6A/E was strongly expressed by colonic epithelial cells from *E. faecalis*-

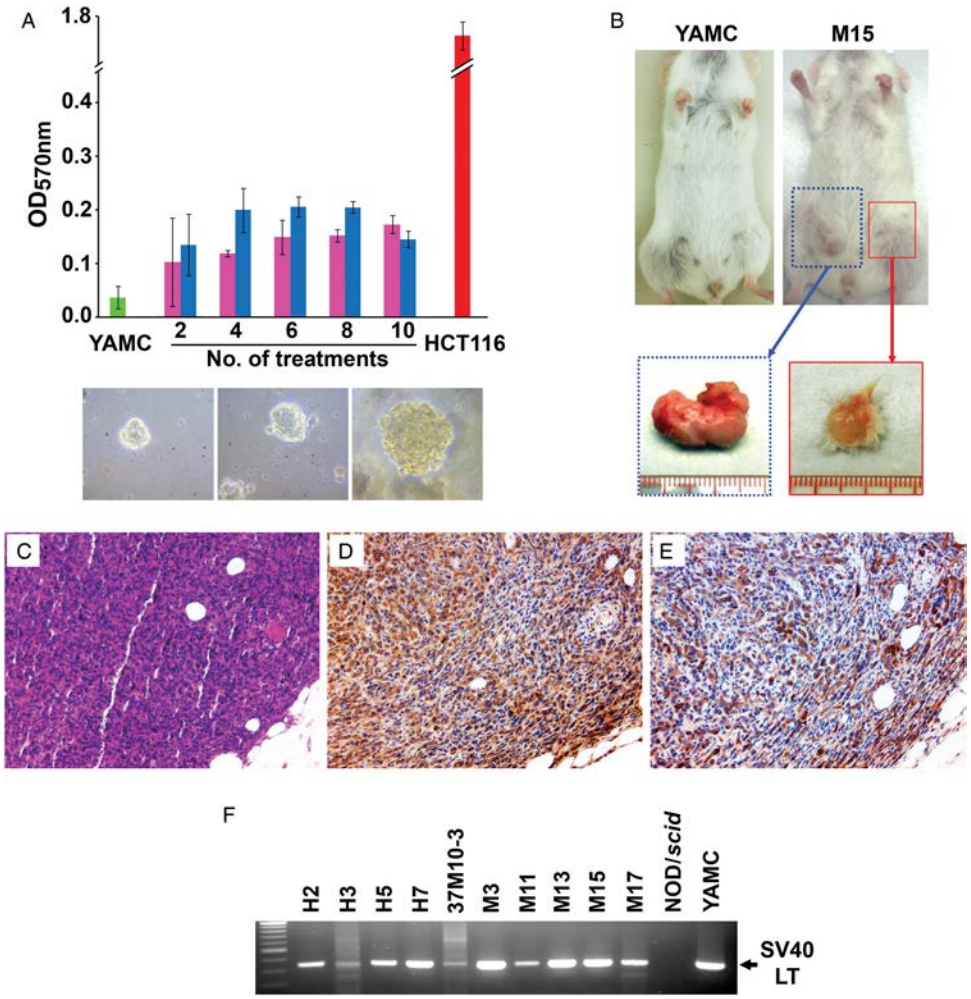

Figure 3 *Enterococcus faecalis*-activated macrophages and 4-hydroxy-2-nonenal (4-HNE) cause cellular transformation. (A) Anchorage-independent growth (*upper graph*) significantly increases for YAMC cells grown in soft agar after two treatments with 1 μM 4-HNE (*pink*) or *E. faecalis*-infected macrophages (*blue*) compared with sham-treated controls (*green*). HCT116 cells are a positive control (*red*). Growth of multicellular spheroids for YAMC cells is evident after 10 treatments with 4-HNE (*middle lower*) or *E. faecalis*-infected macrophages (*left lower*), and as a control following no treatment for HCT116 cells (*right lower*). (B) Allografts grow in flanks of NOD/*scid* mouse injected with clone M15 (*right*) compared with no growth for untreated YAMC cells (*left*); excised tumours for clone M15 (*below*). (C) H&E staining of clone M15 allograft shows poorly differentiated carcinoma (20×). (D) Staining for cytokeratins (brown) confirms epithelial origin (20×). (E) Staining for Dclk1 shows abundant expression of the tumour stem cell antigen (20×). (F) PCR for SV40 large T antigen gene in allografts further confirms YAMC as the cells of origin.

colonised mice (figure 5D, *middle and right*; see online supplementary figure S4B,C). Although Dclk1 was non-differentially expressed in transformed clones, staining for the tumour stem cell marker was positive in numerous epithelial and stromal cells of *E. faecalis*-colonised *Il10*$^{-/-}$ mice (figure 5E). These findings confirm induction of stem/progenitor and tumour stem cell markers in murine allografts and epithelial and stromal cells from biopsies of a BSE-rich tissue microenvironment.

DISCUSSION

The majority of solid tumours, including CRCs, arise from the progressive accumulation of mutations in normal epithelial cells that lead to oncogenic transformation.[1 2] Searches for the origin of mutations that initiate the adenoma-to-carcinoma sequence in CRC have usually focused on exogenous carcinogens or metabolically converted pro-mutagens in foodstuffs. Few studies, however, have investigated endogenous mutagens. This work shows that commensal-polarised macrophages,[10] and a clastogen produced by them, 4-HNE,[13 15] are potent initiators of CIN that lead to the transformation of primary colon epithelial cells through BSE.

BSE has been most thoroughly described following in vivo or in vitro irradiation.[24] This phenomenon is defined by clastogens that diffuse into neighbouring cells to cause CIN. Sophisticated congenic sex-mismatch bone marrow transplant studies have confirmed that BSE occurs in vivo.[25] In addition, BSE is observed in animal models where second primary tumours occur in organs remote from primary sites of carcinogenesis.[26 27] We expanded our understanding of BSE by showing that polarisation of macrophages through infection can also generate this effect.[10 13] Infection-induced BSE and radiation-induced BSE are similar in that both have been linked to COX-2.[8 15 28] *E. faecalis* provides proof-of-principle that human commensals can polarise colonic macrophages to initiate CIN and cellular transformation. This is not meant to imply that other commensal bacteria cannot similarly promote BSE. Indeed, *Escherichia coli*, a Gram-negative bacillus, has been shown to stimulate macrophages to produce 4-HNE in vitro[13] and, much

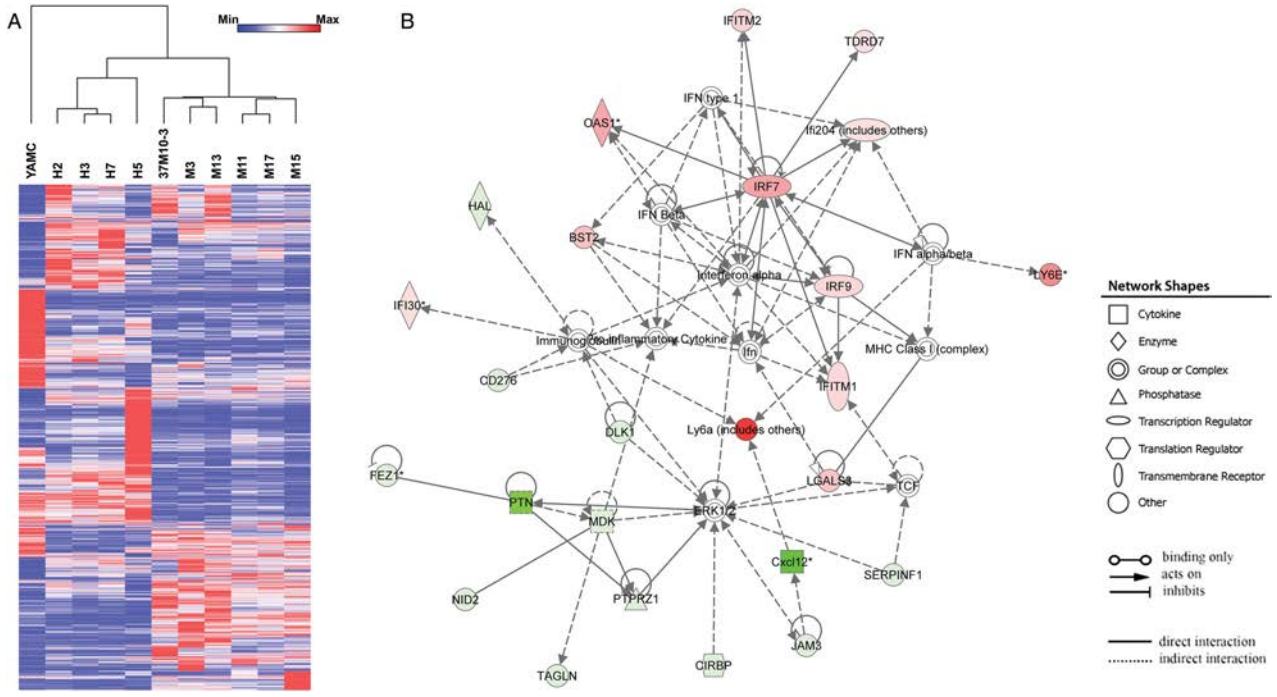

Figure 4 Gene expression in transformed YAMC clones. (A) Heat map shows a total of 2391 probes representing 1974 genes differentially expressed in 10 transformed clones compared with untreated YAMC cells. Dendrogram indicates strong correlations among four clones isolated from 4-HNE-treated YAMC cells and six clones from YAMC cells repetitively exposed to *Enterococcus faecalis*-polarised macrophages. (B) The most highly significant network consists of 25 differentially expressed genes. *Green*, decreased expression; *red*, increased expression.

like *E. faecalis*, a Gram-positive coccus, generate BSE and cellular transformation in colonised *Il10*$^{-/-}$ mice.[7]

Polarised macrophages are found following acute infection, during chronic inflammation and in association with tumours.[12 29] M1 polarised macrophages help clear infections while M2 macrophages assist in parasite clearance and tissue remodelling. Of note, M2 macrophages can also promote the progression of extant cancers.[12] Resting intestinal macrophages are neither M1 nor M2.[11] Instead, under normal conditions, these cells are potently phagocytic but remain non-inflammatory. This distinctive phenotype is a result of the local intestinal microenvironment and helps maintain appropriate homoeostasis and tolerance to commensals. In the *Il10*$^{-/-}$ model, colon macrophages are polarised by colonisation with *E. faecalis* to a M1 phenotype. This phenotype appears essential to BSE.[10] The interaction of polarised macrophages with other immune cells in colorectal carcinogenesis, including mast cells, dendritic cells, T cells or natural killer cells,[5 30–35] is likely

Table 2 Driver genes for cancer in transformed clones

Gene symbol	Classification[2]	Fold-change in gene expression in transformed clones*									
		H2	H3	H5	H7	M3	37M10-3	M11	M13	M15	M17
Arid1b	TSG†	−1.93	−2.04	−1.67	−2.09	−1.89	−1.73	−1.53	−1.80	−1.32	−1.23
Cdkn2a	TSG	−1.01	−1.20	−1.58	−1.01	−3.13	−2.47	−3.51	−2.94	−3.44	−3.57
Daxx	TSG	1.46	1.65	−1.05	1.69	2.43	1.28	1.43	2.25	1.60	1.44
Gata3	TSG	1.10	−.03	−1.68	1.08	1.70	2.52	2.39	1.68	1.65	2.29
Map3k1	TSG	−1.87	−1.42	−1.20	−1.83	−2.42	−3.07	−2.02	−2.64	−1.93	−2.61
Notch1	TSG	2.49	1.69	−1.06	1.35	2.49	3.34	−1.07	3.77	1.23	1.26
Pbrm1	TSG	−1.94	−1.68	−1.33	−2.04	−1.92	−1.58	−1.70	−1.47	1.00	−1.01
Pten	TSG	2.20	1.92	1.80	1.49	1.27	−1.03	1.49	1.53	1.09	1.20
Smad2	TSG	1.01	−1.31	1.08	1.09	−2.21	−2.08	−1.47	−1.86	−1.79	−1.89
Traf7	TSG	−2.08	−1.83	−2.27	−1.59	−1.17	1.12	−1.13	1.10	1.25	−1.09
Egfr	Oncogene	1.25	1.19	−1.31	1.26	−1.66	−2.08	−2.22	−1.56	−3.59	−2.27
Gata2	Oncogene	−1.60	−1.14	−2.01	−1.36	−1.28	1.15	−1.05	1.01	1.21	1.00
Klf4	Oncogene	2.07	2.43	1.70	1.99	2.37	2.31	1.90	1.52	1.86	2.39
Pdgfra	Oncogene	−3.95	−4.18	−3.95	−4.21	−1.37	−1.56	−2.20	−1.59	−2.11	−2.23
Ppp2r1a	Oncogene	−1.76	−1.77	−1.56	−2.04	−1.27	−1.23	−1.38	−1.11	1.00	−1.12
Number of driver genes with ≥ 2.00 fold-change		5	3	3	4	6	7	5	4	3	6

*Red, upregulation; Green, downregulation.
†TSG, tumour suppressor gene.

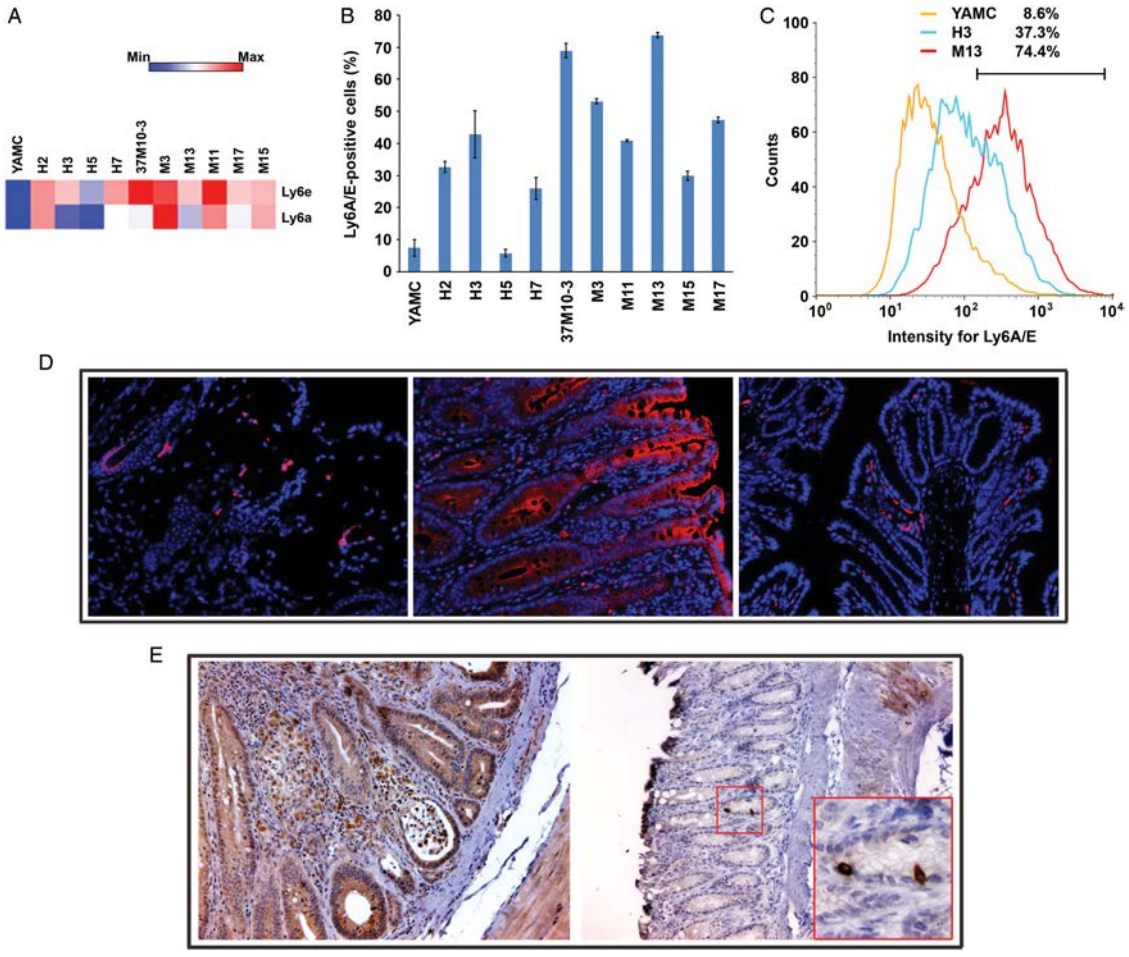

Figure 5 Transformed clones show increased stem/progenitor cell marker expression. (A) Genes for haematopoietic stem/progenitor cell markers *Ly6e* and *Ly6a* are significantly upregulated in transformed clones compared with untreated YAMC cells. (B) The percentage of Ly6A/E-positive cells is increased in 9 out of 10 transformed clones compared with untreated YAMC controls. (C) A representative histogram shows increased Ly6A/E expression in transformed clones H3 and M13 compared with untreated YAMC cells. (D) Immunofluorescent staining shows Ly6A/E-positive cells (*red*) in the M11 allograft tumour (20×, *left*) with nuclei counterstained using 4′,6-diamidino-2-phenylindole (DAPI) (*blue*); inflamed and neoplastic epithelial cells (*middle*) strongly stain for Ly6A/E in colon from *Enterococcus faecalis*-colonised *Il10*$^{-/-}$ mice (20×); no Ly6A/E expression in normal colon epithelia from sham-colonised *Il10*$^{-/-}$ mice (*right*) although a few positively stained immune cells are visible in the lamina propria (20×). (E) Strong staining (brown) for Dclk1 is seen in epithelial and lamina propria cells from inflamed and dysplastic colons of *E. faecalis*-colonised *Il10*$^{-/-}$ mice (20×; *left*); minimal staining is seen in colon biopsies from sham-colonised mice (20×; *right*); inset (60×) shows rare Dclk1^{+} colon crypt cells, most likely representing tuft cells.

important to the regulation of BSE but not yet fully understood and merits additional investigation.

BSE is a plausible theory for sporadic and colitis-associated CRC. It directly addresses the origin of CIN, the most common genotype for these cancers, and links COX-2 reactivity to the initiation of the adenoma-to-carcinoma sequence. In this study, we found that repetitive exposure of primary colon epithelial cells to *E. faecalis*-polarised macrophages or 4-HNE induced aneuploidy and heritable CIN. These findings are consistent with the notion that long-term exposure of epithelial cells to clastogens initiates genomic instability in CRC. Only a minority of our transformed clones did not develop CIN (table 1). Of the many clones that were aneuploid, a majority failed to form tumours in NOD/*scid* mice. We speculate that this is a reflection of the known tumour-suppressive effects of aneuploidy.[36]

Previous studies have shown that CIN and MIN can be induced by specific carcinogens.[37] For example, tissue culture cells surviving near-lethal doses of the exogenous mutagen 2-amino-1-methyl-6-phenylimidazo (4,5-*b*) pyridine acquire CIN.[38] In contrast, cells resistant to treatment with *N*-methyl-*N*′-nitro-*N*-nitrosoguanidine have exhibited MIN. 4-HNE forms bulky adducts[39] and in this study, as with 2-amino-1-methyl-6-phenylimidazo (4,5-*b*) pyridine, was primarily associated with CIN instead of MIN. These findings are consistent with predictions that bulky-adduct-forming mutagens preferentially cause CIN while methylating agents induce MIN.[37] 4-HNE is an α, β-unsaturated aldehyde that readily modifies proteins, forms DNA adducts and contributes to carcinogenesis by inhibiting DNA repair, inducing COX-2, and modulating mitogen-activated protein kinases (MAPK) and nuclear factor (NF)-κB signalling.[14] In addition, 4-HNE causes double-stranded DNA breaks that may help initiate CIN.[9] These breaks are difficult to repair, generate dicentric chromosomes through non-homologous end-joining repair, and result in anaphase bridging.[40] The result can be lagging chromosomes, multipolar mitoses, and missegregation. When bridges fragment, chromosomes enter breakage-fusion-bridge cycles that produce rearrangements and aneuploidy.[40] Finally, 4-HNE also disrupts mitotic

spindles by activating stathmin, a key regulatory protein in microtubule kinetics, and thereby produces microtubule catastrophe.[13] These overlapping mechanisms likely individually and jointly contribute to the initiation of CIN by 4-HNE.

Whole genome sequencing of human cancers has identified ~90 mutations per tumour.[2] Of the many genes affected, only 125 or so 'driver' genes seem important to tumour growth. Typically, two to eight driver mutations are required for malignant transformation.[2 41] In our study, we found differential expression in three to seven driver genes for each transformed clone. In silico analyses detected altered expression in several gene regulators commonly found in cancer (eg, Trim24, Mapk1 and Trp53). We did not investigate, however, whether these changes were due to mutations, copy number alternations, epigenetic modification or disruption of regulatory pathways. Detailed characterisation of mutations and/or regulatory changes in these clones was beyond the scope of this investigation.

Primary epithelial cells from the bladder, cervix, colon, kidney, lung and breast of normal mice can acquire chromosomal aneuploidy and centrosomal instability upon prolonged in vitro passage (eg, 6–12 months).[42] In contrast, the primary murine colon cells in our study were rapidly transformed upon exposure to polarised macrophages or 4-HNE. Techniques for the spontaneous transformation of cells commonly involve a 10-day refeeding protocol that creates nutrient starvation and oxidative/metabolic stresses that likely contribute to genotoxicity. The mechanism(s) for this phenomenon, however, remains to be defined. Our approach involved feeding YAMC cells on a normal schedule (ie, thrice a week) and consisted of only 10 treatments prior to identifying clones that grew as poorly differentiated carcinomas in immunodeficient mice. Unexposed YAMC cells were not transformed. Finally, it should be noted that epithelial tumours do not spontaneously develop in mice, including *Il10*$^{-/-}$ mice, unless carcinogens, inflammation, or changes in oncogenes and/or tumour suppressors are introduced. In contrast, colonisation of *Il10*$^{-/-}$ mice by *E. faecalis* triggers events that generate molecular signatures for BSE and within 6–9 months results in CRC.[10 13]

The expression of Dclk1 for clones that grew as carcinomas in immunodeficient mice was surprising since gene expression analyses failed to identify this gene. This lack of difference in mRNA may reflect regulation by post-translational processing and is an area of ongoing investigation. In addition to Dclk1 expression in allografts, we also found widespread expression in epithelial and stromal cells of dysplastic and cancerous tissues from *E. faecalis*-colonised *Il10*$^{-/-}$ mice. In the normal intestinal epithelium Dclk1 cells appear as fully differentiated epithelial cells and are synonymous with tuft cells.[19 43] These quiescent cells have a long life span, a characteristic likely essential for acquiring multiple mutations as cells undergo transformation. Recent work using the *Apc*$^{Min/+}$ model of intestinal tumorigenesis identified Dclk1-expressing cells as tumour stem cells.[44 45] Deletion of Dclk1 cells resulted in the regression and elimination of intestinal tumours, suggesting that this marker was functionally required for tumour growth. Finally, Dclk1-positive stromal cells in colon biopsies from *E. faecalis*-colonised *Il10*$^{-/-}$ mice may represent cells undergoing the epithelial-mesenchymal transition.[19] This process is defined by a conversion of epithelial cells to divergent phenotypes involved in wound healing, fibrosis and the metastatic spread of cancer. These observations are an area of ongoing investigation.

Another distinctive gene expression signature in transformed clones was Ly6A and Ly6E. These genes are part of a multigene family of glycosyl phosphatidylinositol-anchored cell surface proteins and considered stem/progenitor cell markers.[18] In YAMC cells, members of the Ly6 superfamily are upregulated by interferon-γ, IL-22 and TNFα.[46] Ly6A (or stem cell antigen-1) marks murine haematopoietic stem cells and is involved in cell-cell adhesion and signalling, stem cell self-renewal, and stress responses.[18] It has no human homologue. Notably, overexpression of Ly6A occurs in several murine cancers including prostate and breast.[47 48] Silencing *Ly6a* alters cell proliferation, migration and organisation.[49] Increased expression of Ly6A and Ly6C has been previously reported in colon biopsies from mice with colitis.[46] *Ly6e*, or locus E of the Ly6 multigene family, is an ortholog of *LY6E* in humans and was strongly expressed in nearly all transformed clones. Because *LY6E* is overexpressed in human pancreatic cancer stem cells and CRC,[50] dysregulation of this gene may contribute to tumorigenesis. Finally, as in transformed YAMC clones, we observed marked upregulation of Ly6A/E in colon epithelial cells in *Il10*$^{-/-}$ mice that were colonised with *E. faecalis*.

In summary, repetitive exposure of primary colonic epithelial cells to commensal-polarised macrophages, or the endogenous clastogen 4-HNE, induced CIN, caused transformation via BSE, increased expression of tumour stem cell and stem/progenitor-like markers, and led to the formation of poorly differentiated and invasive tumours in immunodeficient mice. These findings are evidence for commensal-induced endogenous CIN and cellular transformation leading to CRC. Understanding mechanisms by which commensals initiate and promote CRC will permit new preventive strategies for decreasing the incidence of this common human cancer.

Acknowledgements The authors thank Bart Frank at the Oklahoma Medical Research Foundation for gene expression analyses, Ravindranauth Sawh in the Department of Pathology at the University of Oklahoma Health Sciences Center, and Jim Henthorn in the Flow Cytometry Laboratory, and Histology and Immunohistochemistry Core in the Peggy and Charles Stephenson Cancer Center (NIH GM103639).

Contributors MMH provided study supervision; XW and MMH are responsible for study design and concepts, and they analysed data, and wrote the manuscript; XW and YY performed the research.

Funding This study was supported by NIH CA127893 (MMH), Oklahoma Center for the Advancement of Science and Technology HR10-032 (XW), and Francis Duffy Endowment.

Competing interests None.

Provenance and peer review Not commissioned; externally peer reviewed.

Data sharing statement Microarray data has been deposited into Gene Expression Omnibus (Accession number GSE55233). No other unpublished data is available.

REFERENCES

1 Fearon ER. Molecular genetics of colorectal cancer. *Annu Rev Pathol* 2011;6:479–507.
2 Vogelstein B, Papadopoulos N, Velculescu VE, *et al*. Cancer genome landscapes. *Science* 2013;339:1546–58.
3 Boleij A, Tjalsma H. Gut bacteria in health and disease: a survey on the interface between intestinal microbiology and colorectal cancer. *Biol Rev Camb Philos Soc* 2012;87:701–30.
4 Cuevas-Ramos G, Petit CR, Marcq I, *et al*. *Escherichia coli* induces DNA damage in vivo and triggers genomic instability in mammalian cells. *Proc Natl Acad Sci USA* 2010;107:11537–42.
5 Wu S, Rhee KJ, Albesiano E, *et al*. A human colonic commensal promotes colon tumorigenesis via activation of T helper type 17T cell responses. *Nat Med* 2009;15:1016–22.

6 Arthur JC, Perez-Chanona E, Muhlbauer M, *et al*. Intestinal inflammation targets cancer-inducing activity of the microbiota. *Science* 2012;338:120–3.
7 Kim SC, Tonkonogy SL, Albright CA, *et al*. Variable phenotypes of enterocolitis in IL-10 deficient mice monoassociated with two different commensal bacteria. *Gastroenterology* 2005;128:891–906.
8 Wang X, Huycke MM. Extracellular superoxide production by *Enterococcus faecalis* promotes chromosomal instability in mammalian cells. *Gastroenterology* 2007;132:551–61.
9 Wang X, Allen TD, May RJ, *et al*. *Enterococcus faecalis* induces aneuploidy and tetraploidy in colonic epithelial cells through a bystander effect. *Cancer Res* 2008;68:9909–17.
10 Yang Y, Wang X, Huycke T, *et al*. Colon macrophages polarized by commensal bacteria cause colitis and cancer through the bystander effect. *Transl Oncol* 2013;6:596–606.
11 Bain CC, Mowat AM. Intestinal macrophages—specialised adaptation to a unique environment. *Eur J Immunol* 2011;41:2494–8.
12 Murray PJ, Wynn TA. Protective and pathogenic functions of macrophage subsets. *Nat Rev Immunol* 2011;11:723–37.
13 Wang X, Yang Y, Moore DR, *et al*. 4-Hydroxy-2-nonenal mediates genotoxicity and bystander effects caused by *Enterococcus faecalis*-infected macrophages. *Gastroenterology* 2012;142:543–51.
14 Speed N, Blair IA. Cyclooxygenase- and lipoxygenase-mediated DNA damage. *Cancer Metastasis Rev* 2011;30:437–47.
15 Wang X, Allen TD, Yang Y, *et al*. Cyclooxygenase-2 generates the endogenous mutagen *trans*-4-hydroxy-2-nonenal in *Enterococcus faecalis*-infected macrophages. *Cancer Prev Res (Phila)* 2013;6:206–16.
16 Bertagnolli MM, Eagle CJ, Zauber AG, *et al*. Celecoxib for the prevention of sporadic colorectal adenomas. *N Engl J Med* 2006;355:873–84.
17 Thun MJ, Jacobs EJ, Patrono C. The role of aspirin in cancer prevention. *Nat Rev Clin Oncol* 2012;9:259–67.
18 Holmes C, Stanford WL. Concise review: stem cell antigen-1: expression, function, and enigma. *Stem Cells* 2007;25:1339–47.
19 Ong BA, Vega KJ, Houchen CW. Intestinal stem cells and the colorectal cancer microenvironment. *World J Gastroenterol* 2014;20:1898–909.
20 Whitehead RH, VanEeden PE, Noble MD, *et al*. Establishment of conditionally immortalized epithelial cell lines from both colon and small intestine of adult H-2Kb-tsA58 transgenic mice. *Proc Natl Acad Sci USA* 1993;90:587–91.
21 Yang Y, Wang X, Moore DR, *et al*. TNF-α mediates macrophage-induced bystander effects through netrin-1. *Cancer Res* 2012;72:5219–29.
22 Beroukhim R, Mermel CH, Porter D, *et al*. The landscape of somatic copy-number alteration across human cancers. *Nature* 2010;463:899–905.
23 Chiu PP, Ivakine E, Mortin-Toth S, *et al*. Susceptibility to lymphoid neoplasia in immunodeficient strains of nonobese diabetic mice. *Cancer Res* 2002;62:5828–34.
24 Lorimore SA, Wright EG. Radiation-induced genomic instability and bystander effects: related inflammatory-type responses to radiation-induced stress and injury? A review. *Int J Radiat Biol* 2003;79:15–25.
25 Watson GE, Lorimore SA, Macdonald DA, *et al*. Chromosomal instability in unirradiated cells induced in vivo by a bystander effect of ionizing radiation. *Cancer Res* 2000;60:5608–11.
26 Westbrook AM, Wei B, Braun J, *et al*. Intestinal mucosal inflammation leads to systemic genotoxicity in mice. *Cancer Res* 2009;69:4827–34.
27 Rao VP, Poutahidis T, Ge Z, *et al*. Innate immune inflammatory response against enteric bacteria *Helicobacter hepaticus* induces mammary adenocarcinoma in mice. *Cancer Res* 2006;66:7395–400.
28 Zhou H, Ivanov VN, Gillespie J, *et al*. Mechanism of radiation-induced bystander effect: role of the cyclooxygenase-2 signaling pathway. *Proc Natl Acad Sci USA* 2005;102:14641–6.
29 Lu H, Ouyang W, Huang C. Inflammation, a key event in cancer development. *Mol Cancer Res* 2006;4:221–33.
30 Gounaris E, Erdman SE, Restaino C, *et al*. Mast cells are an essential hematopoietic component for polyp development. *Proc Natl Acad Sci USA* 2007;104:19977–82.
31 Vivier E, Ugolini S, Blaise D, *et al*. Targeting natural killer cells and natural killer T cells in cancer. *Nat Rev Immunol* 2012;12:239–52.
32 Garrett WS, Punit S, Gallini CA, *et al*. Colitis-associated colorectal cancer driven by T-bet deficiency in dendritic cells. *Cancer Cell* 2009;16:208–19.
33 Grivennikov SI, Wang K, Mucida D, *et al*. Adenoma-linked barrier defects and microbial products drive IL-23/IL-17-mediated tumour growth. *Nature* 2012;491:254–8.
34 Gounaris E, Blatner NR, Dennis K, *et al*. T-regulatory cells shift from a protective anti-inflammatory to a cancer-promoting proinflammatory phenotype in polyposis. *Cancer Res* 2009;69:5490–7.
35 Erdman SE, Sohn JJ, Rao VP, *et al*. $CD4^+CD25^+$ regulatory lymphocytes induce regression of intestinal tumors in $Apc^{Min/+}$ mice. *Cancer Res* 2005;65:3998–4004.
36 Weaver BA, Silk AD, Montagna C, *et al*. Aneuploidy acts both oncogenically and as a tumor suppressor. *Cancer Cell* 2007;11:25–36.
37 Breivik J, Gaudernack G. Genomic instability, DNA methylation, and natural selection in colorectal carcinogenesis. *Cancer Biol* 1999;9:245–54.
38 Bardelli A, Cahill DP, Lederer G, *et al*. Carcinogen-specific induction of genetic instability. *Proc Natl Acad Sci USA* 2001;98:5770–5.
39 Uchida K. 4-Hydroxy-2-nonenal: a product and mediator of oxidative stress. *Prog Lipid Res* 2003;42:318–43.
40 Acilan C, Potter DM, Saunders WS. DNA repair pathways involved in anaphase bridge formation. *Genes Chromosomes Cancer* 2007;46:522–31.
41 Wood LD, Parsons DW, Jones S, *et al*. The genomic landscapes of human breast and colorectal cancers. *Science* 2007;318:1108–13.
42 Padilla-Nash HM, McNeil NE, Yi M, *et al*. Aneuploidy, oncogene amplification and epithelial to mesenchymal transition define spontaneous transformation of murine epithelial cells. *Carcinogenesis* 2013;34:1929–39.
43 Gerbe F, van Es JH, Makrini L, *et al*. Distinct ATOH1 and Neurog3 requirements define tuft cells as a new secretory cell type in the intestinal epithelium. *J Cell Biol* 2011;192:767–80.
44 Westphalen CB, Asfaha S, Hayakawa Y, *et al*. Long-lived intestinal tuft cells serve as colon cancer-initiating cells. *J Clin Invest* 2014;124:1283–95.
45 Nakanishi Y, Seno H, Fukuoka A, *et al*. Dclk1 distinguishes between tumor and normal stem cells in the intestine. *Nat Genet* 2012;45:98–103.
46 Flanagan K, Modrusan Z, Cornelius J, *et al*. Intestinal epithelial cell up-regulation of LY6 molecules during colitis results in enhanced chemokine secretion. *J Immunol* 2008;180:3874–81.
47 Xin L, Lawson DA, Witte ON. The Sca-1 cell surface marker enriches for a prostate-regenerating cell subpopulation that can initiate prostate tumorigenesis. *Proc Natl Acad Sci USA* 2005;102:6942–7.
48 Li Y, Welm B, Podsypanina K, *et al*. Evidence that transgenes encoding components of the Wnt signaling pathway preferentially induce mammary cancers from progenitor cells. *Proc Natl Acad Sci USA* 2003;100:15853–8.
49 Batts TD, Machado HL, Zhang Y, *et al*. Stem cell antigen-1 (sca-1) regulates mammary tumor development and cell migration. *PLoS ONE* 2011;6:e27841.
50 Bresson-Mazet C, Gandrillon O, Gonin-Giraud S. Stem cell antigen 2: a new gene involved in the self-renewal of erythroid progenitors. *Cell Prolif* 2008;41:726–38.

Supplementary Figure Legends

Figure S1. Analysis of mismatch repair gene products. (A) Western blots for MSH2, a key mismatch repair protein, in selected clones from YAMC treated with 4-HNE (*upper panel*) or *E. faecalis*-infected macrophages (*lower panel*). (B) MSH2 increases in all clones, except clone H5, compared with parental YAMC cells after being normalized to β-actin.

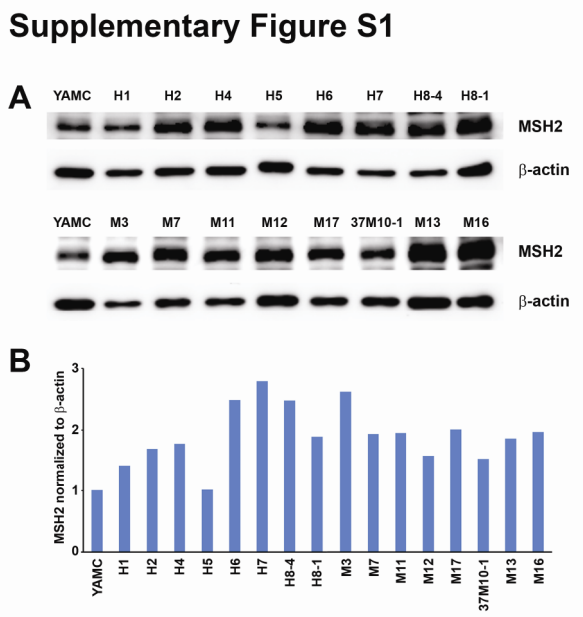

Figure S2. Xenograft assay of HCT116 as a positive control. (A) Large tumors are seen in the flanks of HCT116-injected NOD/*scid* mouse (*arrows*). (B) Excised tumors from HCT116-injected NOD/*scid* mouse. (C) H & E staining for xenograft tumor shows poorly differentiated carcinomas (20X). (D) Immunohistochemical staining for cytokeratin 20 confirmed carcinoma in xenograft (40X).

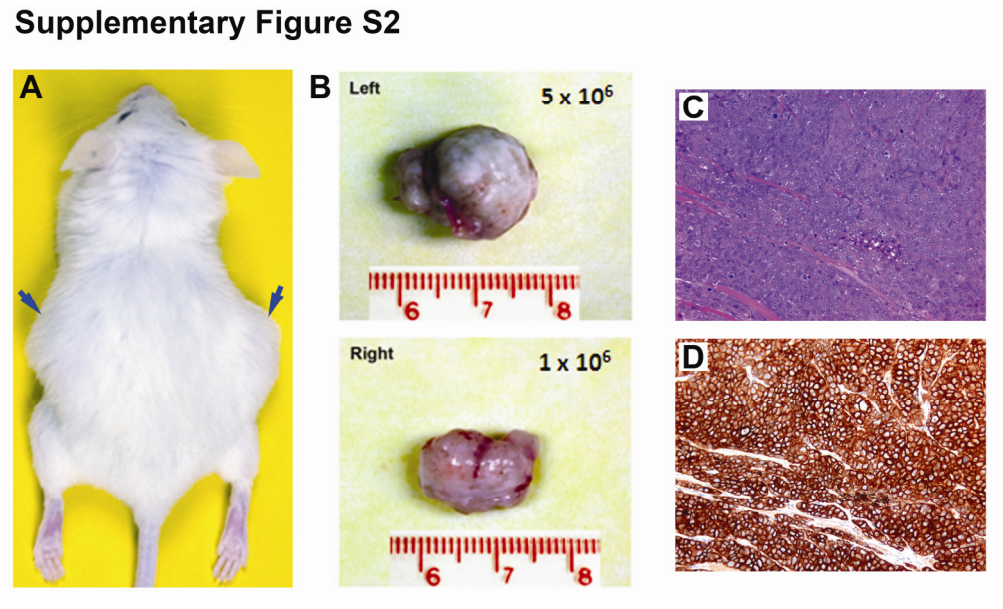

Figure S3. Allograft assay of YAMC-derived clones. (A) A small tumor is noted in a NOD/*scid* mouse following 20 weeks of subcutaneous injection with 5×10^6 M17 cells in the medium free of matrigel. (B) Excised tumor. (C) H & E staining shows poorly differentiated carcinoma (20X). (D) PCR for SV40 large T antigen gene confirms that tumor is originated from YAMC cells. (E) Staining shows poorly differentiated carcinoma (*blue arrows*) invading skin (*green arrows*, hair follicles). (F) H&E staining shows poorly differentiated carcinoma (*blue arrows*) invading muscle (*yellow arrows*).

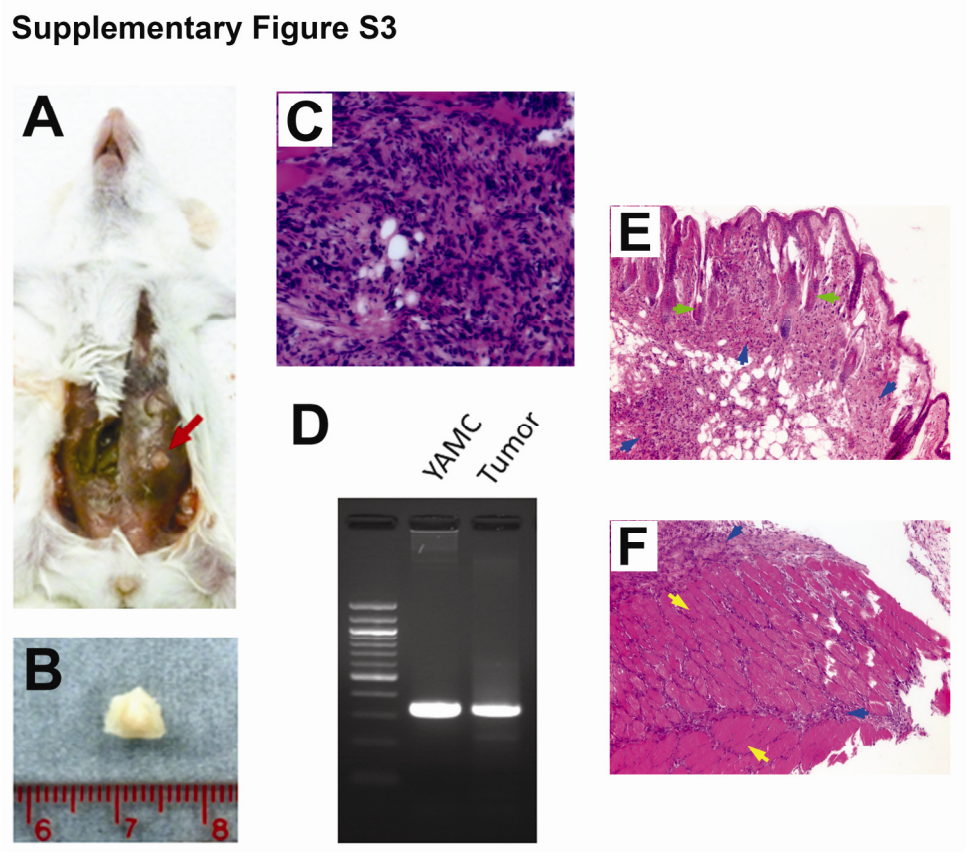

Figure S4. Immunohistochemical staining for Ly6A/E. (A) Ly6A/E-positive cells (*arrows*) are evident in allograft tumor of M11-injected NOD/*scid* mouse (20X). (B) Colonic epithelial cells are strongly stained for Ly6A/E in the areas of inflammation and neoplasia of colon biopsies from *E. faecalis*-colonized *Il10*$^{-/-}$ mice (20X). (C) No Ly6A/E expression is seen in normal epithelial cells from sham-colonized *Il10*$^{-/-}$ mice. Several immune cells in the lamina propria, however, are positively stained for Ly6A/E in these mice (20X).

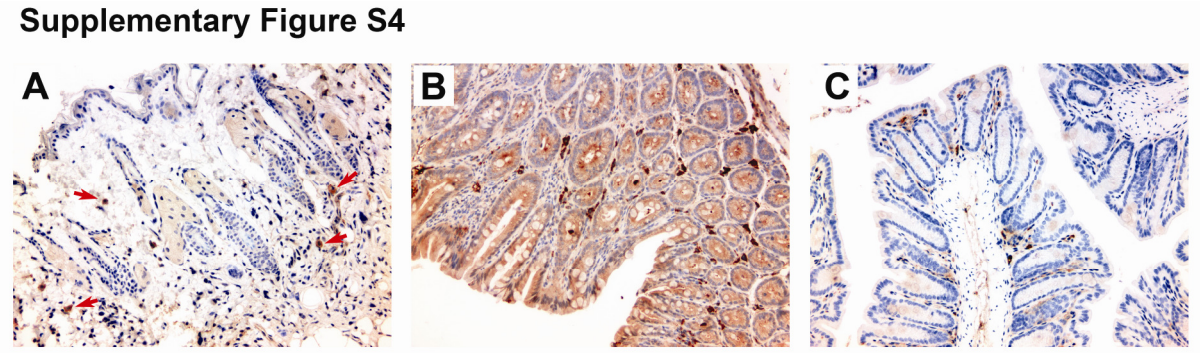

Table S1. Differentially expressed genes (≥ 2.0 fold-change) in transformed clones for Ingenuity Pathway Analysis.

Symbol*	Name	Geom mean of intensities in AllExp	Geom mean of intensities in Cntl	Fold-change AllExp v Cntl
Ly6a	lymphocyte antigen 6 complex, locus A (Ly6a)	3459.91	241.21	14.344
Cdkn1a	cyclin-dependent kinase inhibitor 1A (P21) (Cdkn1a)	2653.67	283.33	9.366
Anxa8	annexin A8 (Anxa8)	1769.99	201.3	8.793
Anxa8	annexin A8 (Anxa8)	1643.92	201.4	8.162
Ly6e		7597.81	942.86	8.058
LOC100038882	PREDICTED: hypothetical protein LOC100038882 (LOC100038882)	8113.77	1026.19	7.907
Cdkn1a	cyclin-dependent kinase inhibitor 1A (P21) (Cdkn1a)	6350.65	810.62	7.834
Ly6e	lymphocyte antigen 6 complex, locus E (Ly6e)	3308.57	428.16	7.727
Dnali1		847.82	123.07	6.889
Irf7	interferon regulatory factor 7 (Irf7)	1017.71	161.95	6.284
Oas1g	2'-5' oligoadenylate synthetase 1G (Oas1g)	3235.96	549.33	5.891
Oas1g	2'-5' oligoadenylate synthetase 1G (Oas1g)	1525.74	297.97	5.120
Apol9b	apolipoprotein L 9b (Apol9b)	2060.57	403.99	5.101
Ephx1	epoxide hydrolase 1, microsomal (Ephx1)	3226.02	651.91	4.949
6530402F18Rik		562.92	117.51	4.790
LOC223672		4372.4	929.09	4.706
Capg	capping protein (actin filament), gelsolin-like (Capg), transcript variant 1	1175.06	257.51	4.563
Trp53inp1	transformation related protein 53 inducible nuclear protein 1 (Trp53inp1)	1959.4	452.54	4.330
Fam134b	family with sequence similarity 134, member B (Fam134b), transcript variant 2	724.96	173.3	4.183
Bst2	bone marrow stromal cell antigen 2 (Bst2)	2738.66	658.89	4.156
Lgals3	lectin, galactose binding, soluble 3 (Lgals3)	7860.48	1921.47	4.091
Car13	carbonic anhydrase 13 (Car13)	1127.91	300.25	3.757
2210023G05Rik	RIKEN cDNA 2210023G05 gene (2210023G05Rik)	1582.82	423.2	3.740
Ak1	adenylate kinase 1 (Ak1)	961.3	261.58	3.675
Ccng1	cyclin G1 (Ccng1)	6384.15	1808.89	3.529
D12Ertd647e	DNA segment, Chr 12, ERATO Doi 647, expressed (D12Ertd647e), transcript variant 4	7607.3	2428.97	3.132
D12Ertd647e	DNA segment, Chr 12, ERATO Doi 647, expressed (D12Ertd647e), transcript variant 5	6887.52	2209.86	3.117
Sqrdl	sulfide quinone reductase-like (yeast) (Sqrdl)	510.39	169.95	3.003
Ifitm3	interferon induced transmembrane protein 3 (Ifitm3)	11505.6	3864.62	2.977
A330089M16Rik		345.61	118.59	2.914
Pde3a		312.92	107.45	2.912
H2-T23	histocompatibility 2, T region locus 23 (H2-T23)	820.86	290.26	2.828
Irf9	interferon regulatory factor 9 (Irf9)	1109.91	401.34	2.766
Ifitm1	interferon induced transmembrane protein 1 (Ifitm1)	11647.61	4415.68	2.638
Coro1b	coronin, actin binding protein 1B (Coro1b)	3655.52	1388.93	2.632
Fxyd5	FXYD domain-containing ion transport regulator 5 (Fxyd5)	482.22	187.45	2.573
Lynx1	Ly6/neurotoxin 1 (Lynx1)	333.02	134.73	2.472
Gsdmdc1	gasdermin domain containing 1 (Gsdmdc1)	600.77	247.38	2.429
Gsdmdc1	gasdermin domain containing 1 (Gsdmdc1)	2484.51	1023.12	2.428
LOC100047963	PREDICTED: similar to ADIR1 (LOC100047963)	1338.77	568.37	2.355
scl0001379.1_70		448.96	190.92	2.352

LOC100044430	PREDICTED: similar to Interferon activated gene 205 (LOC100044430)	706.3	301	2.347
Ifi30	interferon gamma inducible protein 30 (Ifi30)	897.22	391.25	2.293
Ggta1	glycoprotein galactosyltransferase alpha 1, 3 (Ggta1)	445.66	194.68	2.289
Dhrs7	dehydrogenase/reductase (SDR family) member 7 (Dhrs7)	1062.82	470.24	2.260
EG433865	PREDICTED: predicted gene, EG433865 (EG433865)	917	408.53	2.245
St3gal2	ST3 beta-galactoside alpha-2,3-sialyltransferase 2 (St3gal2), transcript variant 2	713.98	320.45	2.228
Tdrd7	tudor domain containing 7 (Tdrd7)	1442.82	649.42	2.222
Actb	actin, beta, cytoplasmic (Actb)	2099.32	953.95	2.201
Mlkl	mixed lineage kinase domain-like (Mlkl) XM_924589	2327.26	1061.25	2.193
Tspo	translocator protein (Tspo)	3682.07	1685.41	2.185
LOC100047261	PREDICTED: similar to spermidine/spermine N1-acetyltransferase (LOC100047261), misc RNA.	2692.75	1239.31	2.173
Trim47	tripartite motif-containing 47 (Trim47)	532.06	246.19	2.161
Fbxo6	F-box protein 6 (Fbxo6)	2408.36	1118.16	2.154
Actb	actin, beta (Actb)	1935.11	902.48	2.144
Ddx60	DEAD (Asp-Glu-Ala-Asp) box polypeptide 60 (Ddx60)	301.87	141.38	2.135
Arsa	arylsulfatase A (Arsa)	1536.34	720.1	2.134
LOC100046469	PREDICTED: similar to Plec1 protein, transcript variant 1 (LOC100046469)	311.62	146.43	2.128
4732458O05Rik		739.23	349.99	2.112
Klf4	Kruppel-like factor 4 (gut) (Klf4)	511.31	244.53	2.091
Tspo	translocator protein (Tspo)	3653.66	1752.05	2.085
Gsdmdc1	gasdermin domain containing 1 (Gsdmdc1)	989.09	474.6	2.084
Adfp	adipose differentiation related protein (Adfp)	495.37	238.46	2.077
LOC100046469	PREDICTED: similar to Plec1 protein, transcript variant 1 (LOC100046469)	297.84	144.79	2.057
Txnip	thioredoxin interacting protein (Txnip), transcript variant 1	1205.52	588.87	2.047
Ostf1	osteoclast stimulating factor 1 (Ostf1)	2024.89	999.75	2.025
Ifi204	interferon activated gene 204 (Ifi204)	526.61	261.34	2.015
Ifi30	interferon gamma inducible protein 30 (Ifi30)	446.48	221.79	2.013
Txnip	thioredoxin interacting protein (Txnip), transcript variant 2	2023.78	1008.19	2.007
Plec1	plectin 1 (Plec1), transcript variant 11	642.3	320.33	2.005
Avpr1a	arginine vasopressin receptor 1A (Avpr1a)	119.45	239.23	-2.003
Stx11	PREDICTED: syntaxin 11 (Stx11)	476.09	962.23	-2.021
LOC674960	PREDICTED: similar to high-mobility group box 1 (LOC674960), misc RNA.	207.59	423.13	-2.038
Cdh3		236.11	481.91	-2.041
Epha1	Eph receptor A1 (Epha1)	152.84	312.81	-2.047
9030624G23Rik	PREDICTED: RIKEN cDNA 9030624G23 gene (9030624G23Rik)	209.44	429.74	-2.052
Odf2	outer dense fiber of sperm tails 2 (Odf2)	176.63	362.96	-2.055
Gpr23		120.58	248.34	-2.060
Plac1	placental specific protein 1 (Plac1)	144.78	301.93	-2.085
Rhobtb1	Rho-related BTB domain containing 1 (Rhobtb1)	149.14	311.12	-2.086
Dlg3	discs, large homolog 3 (Drosophila) (Dlg3)	184.06	384.19	-2.087
Il16	interleukin 16 (Il16)	119.14	248.84	-2.089
Emb	embigin (Emb)	112.55	235.47	-2.092
Syngr1	synaptogyrin 1 (Syngr1), transcript variant 1b	131.19	274.58	-2.093
Gstm5	glutathione S-transferase, mu 5 (Gstm5)	645.4	1353.64	-2.097
Ttc28	PREDICTED: tetratricopeptide repeat domain 28 (Ttc28)	163.9	344.43	-2.101

OTTMUSG00000004461	predicted gene, OTTMUSG00000004461 (OTTMUSG00000004461)	283.31	596.28	-2.105
scl0002255.1_1		112.54	236.88	-2.105
Ipo5	importin 5 (Ipo5)	734.9	1561.97	-2.125
4932408C11Rik		114.17	243.49	-2.133
Nfib		225.47	486.74	-2.159
0610007N19Rik	PREDICTED: RIKEN cDNA 0610007N19 gene (0610007N19Rik)	193.4	417.94	-2.161
Odz3	odd Oz/ten-m homolog 3 (Drosophila) (Odz3)	201.81	440.42	-2.182
Fez1	fasciculation and elongation protein zeta 1 (zygin I) (Fez1)	148.41	324.42	-2.186
Gpx7	glutathione peroxidase 7 (Gpx7)	113.21	250.59	-2.213
Spnb2	spectrin beta 2 (Spnb2), transcript variant 2	470.32	1045.74	-2.223
Myh10	myosin, heavy polypeptide 10, non-muscle (Myh10)	684.26	1529.88	-2.236
5730525O22Rik		430.32	969.43	-2.253
D17H6S56E-5	DNA segment, Chr 17, human D6S56E 5 (D17H6S56E-5)	186.87	423.51	-2.266
Ptprz1	protein tyrosine phosphatase, receptor type Z, polypeptide 1 (Ptprz1)	125.27	284.11	-2.268
Epm2aip1	EPM2A (laforin) interacting protein 1 (Epm2aip1)	264.3	600.86	-2.273
LOC382555		1230.93	2813.45	-2.286
Dmrta2	doublesex and mab-3 related transcription factor like family A2 (Dmrta2)	137.06	313.52	-2.287
AI448196		114.48	263.81	-2.304
Zfp703	PREDICTED: zinc finger protein 703 (Zfp703)	391.4	902.42	-2.306
Serping1		119.48	276.16	-2.311
4931406P16Rik	RIKEN cDNA 4931406P16 gene (4931406P16Rik)	677.59	1572.48	-2.321
scl0002507.1_236		200.88	468.46	-2.332
Gpc2	glypican 2 (cerebroglycan) (Gpc2)	120.71	283.55	-2.349
B3galnt1	UDP-GalNAc:betaGlcNAc beta 1,3-galactosaminyltransferase, polypeptide 1 (B3galnt1)	116.04	273.84	-2.360
Jam3	junction adhesion molecule 3 (Jam3)	174.99	412.96	-2.360
Trim27		164.85	390.33	-2.368
C130020C13Rik		290.18	688.75	-2.374
Id4	inhibitor of DNA binding 4 (Id4)	137.36	326.52	-2.377
1700007G11Rik	RIKEN cDNA 1700007G11 gene (1700007G11Rik)	135.21	322.38	-2.384
Fez1	fasciculation and elongation protein zeta 1 (zygin I) (Fez1)	139.52	333.3	-2.389
Hnrpdl	heterogeneous nuclear ribonucleoprotein D-like (Hnrpdl)	738.22	1799.3	-2.437
Cd276	CD276 antigen (Cd276)	166.19	406.02	-2.443
Stard10	START domain containing 10 (Stard10)	307.04	757.47	-2.467
6330406I15Rik	RIKEN cDNA 6330406I15 gene (6330406I15Rik)	166.71	412.7	-2.476
6330406I15Rik	RIKEN cDNA 6330406I15 gene (6330406I15Rik)	195.57	495.49	-2.534
Tacstd2	tumor-associated calcium signal transducer 2 (Tacstd2)	153.81	392.36	-2.551
Cirbp	cold inducible RNA binding protein (Cirbp)	409.68	1074.94	-2.624
scl0003131.1_3		153.72	423.07	-2.752
1110003F05Rik		157.63	437.68	-2.777
Gstk1	glutathione S-transferase kappa 1 (Gstk1)	139.38	389.34	-2.793
Wipf1	WAS/WASL interacting protein family, member 1 (Wipf1)	136.35	393.6	-2.887
Serping1	serine (or cysteine) peptidase inhibitor, clade G, member 1 (Serping1)	121.56	353.11	-2.905
LOC226017		117.03	345.25	-2.950
Tagln	transgelin (Tagln)	166.59	493.83	-2.964
Capn6	calpain 6 (Capn6)	128.03	383.66	-2.997
Myl9	PREDICTED: myosin, light polypeptide 9, regulatory (Myl9)	129.58	390.16	-3.011
Mex3a	mex3 homolog A (C. elegans) (Mex3a)	213.27	654.17	-3.067

Srpx	sushi-repeat-containing protein (Srpx)	109.82	341.53	-3.110
Ddx25	DEAD (Asp-Glu-Ala-Asp) box polypeptide 25 (Ddx25)	148.63	463.87	-3.121
Hal	histidine ammonia lyase (Hal)	137.09	432.99	-3.158
Zfp521	zinc finger protein 521 (Zfp521), transcript variant 2	141.01	447.51	-3.174
Igf2bp3		183.29	607.5	-3.314
Runx1t1	runt-related transcription factor 1; translocated to, 1 (cyclin D-related) (Runx1t1)	130.59	436.55	-3.343
ORF63	open reading frame 63 (ORF63)	151.84	521.34	-3.433
Nid2	nidogen 2 (Nid2)	172.18	601.87	-3.496
9430052C07Rik		199.83	728.58	-3.646
Mdk	midkine (Mdk), transcript variant 3	129.78	473.63	-3.649
Dlk1	delta-like 1 homolog (Drosophila) (Dlk1)	118.1	439.12	-3.718
Gstk1	glutathione S-transferase kappa 1 (Gstk1)	164.83	617.04	-3.743
Asphd2	aspartate beta-hydroxylase domain containing 2 (Asphd2)	138.1	524.37	-3.797
Igf2	insulin-like growth factor 2 (Igf2)	143.14	552.37	-3.859
Serpinf1	serine (or cysteine) peptidase inhibitor, clade F, member 1 (Serpinf1)	178.21	688.69	-3.864
Grb10		1774.18	7351.32	-4.144
Gm22	PREDICTED: gene model 22, (NCBI) (Gm22)	153.24	638.28	-4.165
Fgf5	fibroblast growth factor 5 (Fgf5)	505.61	2138	-4.229
Armcx1	armadillo repeat containing, X-linked 1 (Armcx1)	135.78	578.19	-4.258
Podxl2	podocalyxin-like 2 (Podxl2)	128.65	565.65	-4.397
Limch1	LIM and calponin homology domains 1 (Limch1)	121	575.33	-4.755
6330404C01Rik		140.77	692.04	-4.916
1700048O20Rik		137.09	681.52	-4.971
Prkg1		137.04	725.13	-5.291
Zic1	zinc finger protein of the cerebellum 1 (Zic1)	140	822.89	-5.878
EG433229	PREDICTED: predicted gene, EG433229, transcript variant 7 (EG433229)	165.76	1010.61	-6.097
Mmp2	matrix metallopeptidase 2 (Mmp2)	339.09	2992.32	-8.825
Sfrp2	secreted frizzled-related protein 2 (Sfrp2)	329.33	4098.72	-12.446
Cxcl12	chemokine (C-X-C motif) ligand 12 (Cxcl12), transcript variant 3	138.6	1903.43	-13.733
Cxcl12	chemokine (C-X-C motif) ligand 12 (Cxcl12), transcript variant 1	127.73	3105.6	-24.314
Ptn	pleiotrophin (Ptn)	120.37	5835.39	-48.479
Cxcl12		137.3	9349	-68.092

*Highlighted genes were identified with multiple probes.

Table S2. Gene networks for differentially expressed genes in transformed clones by Ingenuity Pathway Analysis.

ID	Molecules in Network	Score*	No. of Focus Molecules§	Top Functions
1	BST2, CD276, CIRBP, Cxcl12, DLK1, ERK1/2, FEZ1, HAL, IFI30, Ifi204 (includes others), IFITM1, IFITM2, Ifn, IFN alpha/beta, IFN Beta, IFN type 1, Immunoglobulin, Interferon alpha, IRF7, IRF9, JAM3, LGALS3, Ly6a (includes others), LY6E, MDK, MHC Class I (complex), NID2, OAS1, Pro-inflammatory Cytokine, PTN, PTPRZ1, SERPINF1, TAGLN, TCF, TDRD7	53	25	Infectious Disease, Cardiovascular System Development and Function, Cell Morphology
2	ACTB, Actin, Akt, Alp, Alpha catenin, CAPG, CCNG1, CDH3, Collagen type IV, Collagen(s), Cyclin E, F Actin, FGF5, FXYD5, GRB10, Growth hormone, IGF2, KLF4, Laminin, LDL, MMP2, MYH10, MYL9, NFAT (complex), Notch, OSTF1, Pdgf (complex), PDGF BB, PLAC1, PRKG1, Rock, SERPING1, TACSTD2, Tgf beta, WIPF1	35	18	Organ Morphology, Reproductive System Development and Function, Cellular Growth and Proliferation
3	Ap1, caspase, CD3, CDKN1A, Cg, Ck2, Creb, Cyclin A, cytochrome C, DDX25, EMB, estrogen receptor, FSH, glutathione peroxidase, GPX7, GSTK1, GSTM3, Hdac, Histone h3, Histone h4, ID4, IGF2BP3, Igm, IL16, MLKL, NFkB (complex), PDE3A, PI3K (complex), Rb, RUNX1T1, SFRP2, STARD10, TP53INP1, TSPO, TXNIP	32	17	Cell Cycle, Connective Tissue Development and Function, Inflammatory Disease
4	AGRN, Apol9a/Apol9b, ARMCX5-GPRASP2/GPRASP2, BST2, CRIPT, CSTA, DDX60, DLG3, EPHA1, EPHX1, EPM2AIP1, GLI2, HTR4, IFI35, IFI44, IPO5, MSX2, N4BP3, NFIB, PARP12, PLAC8, PODXL2, PSMB10, PTH1R, RHOBTB1, S100A11, SQRDL, TAF1D, TPX2, TRIM24, TRIM47, UBC, ZIC1, ZIC2, ZNF521	28	15	Cancer, Embryonic Development, Nervous System Development and Function
5	AGRN, AK1, ANXA8L2 (includes others), APP, ARSA, BLOC1S1, calpain, CAPN6, CASP3, chondroitin sulfate A, Cxcl12, DHRS7, DMRTA2, DNALI1, EIF3F, ENG, ESR1, FAM3B, FBXO6, FKBPL, HNRPDL, IL16, Ly6a (includes others), MEX3A, NRP1, PABPC1, PRTN3, RYR1, SRPX, STC2, SUZ12, TCN2, TGFB1, TLL1, ZNF703	26	15	Cellular Movement, Hematological System Development and Function, Immune Cell Trafficking
6	androstenediol, APP, ARMCX1, B3GALNT1, BCL2, BMPR2, C4orf22, CCR2, CDH13, CDK4, CLDN3, CTSF, Cxcl12, ENG, ENO2, ESR2, FAM134B, GADD45G, HAVCR2, LIMCH1, LUC7L2, LYNX1, MDK, MMP15, NFKBIA, NQO2, NRP1, ODF2, progesterone, RASSF3, ST3GAL2, SYNGR1, TP53BP2, Ttc28, UBQLN1	20	12	Hematological System Development and Function, Tissue Morphology, Cellular Movement
7	ADAM10, ADD2, AVPR1A, CCR2, CORO1B, CSF3R, ERK, Focal adhesion kinase, FTL, Ggta1, HLA-E, HTR4, IgG, IL1, IL16, Insulin, Jnk, Ly6a (includes others), Mapk, NRP1, P38 MAPK, Pkc(s), PTPRZ1, Rap1, Ras,Ras homolog, RYR1, S100A12, Sos, SP7, STX11, TCR, TRIM27, Ubiquitin, Vegf	14	9	Infectious Disease, Cell Morphology, Hematological System Development and Function
8	GPC2, GSTP1	2	1	Cancer, Lipid Metabolism, Small Molecule Biochemistry

***Score:** The score is derived from a p-value and indicates the likelihood of the Focus Molecules in a network being found together due to random chance. A score of 2 indicates that there is a 1 in 100 chance that the Focus Molecules are together in a network due to random chance. Therefore, scores of 2 or higher have at least a 99% confidence of not being generated by random chance alone (Long et al., *In Silico Biol.* 2004, 4: 0033).
§Focus Molecules: Molecules that are from uploaded list, pass filters are applied, and are available for generating networks.